Electronic Supplementary Information

For

NH_3/H_2O-mediated proton conductivity and photocatalytic behaviour of Fe(II)-hydroxyphosphonoacetate and M(II)-substituted derivatives

Inés R. Salcedo,[a] Montse Bazaga-García,[a] Ana Cuesta,[a] Enrique R. Losilla,[a] Konstantinos D. Demadis,[b] Pascual Olivera-Pastor,[a] Rosario M.P. Colodrero,[c*] Aurelio Cabeza[a*]

[a]*Departamento de Química Inorgánica, Universidad de Málaga, Campus Teatinos s/n, Málaga-29071, Spain; Tel: +34 952131874; E-mail: aurelio@uma.es*

[b]*Crystal Engineering, Growth and Design Laboratory, Department of Chemistry, University of Crete, Voutes Campus, Crete GR-71003, Greece.*

[c]*Faculty of Science & Engineering, University of Wolverhampton, Wulfruna Street, Wolverhampton WV1 1LY, UK.; E-mail: r.perezcolodrero@wlv.ac.uk*

Table of contents:

Figures:

Figure S5. Phase identification for compounds **Fe_xM_{1-x}-HPAA (M^{2+}=Co, Zn)** calcined at 1000 °C under (a) N_2 or (b) H_2 atmospheres.

Figure S6. Rietveld plots for **$Fe[HO_3PCH(OH)CO_2]\cdot(NH_3)_x\cdot(H_2O)_y$ (Fe-NH_3-xh).**

Figure S7. X-ray Pair Distribution Function (PDF) analysis. Observed (blue symbol) and calculated (red line) PDF patterns of **Fe-HPAA** (a), **Fe-NH_3-36h** (b), **Fe-NH_3-48h** (c) in the range 1.4-10 Å (left) and 10-50 Å (right).

Figure S8. TG and DTA curves for compounds **Fe-HPAA** (a) and **Fe-NH_3-72h** (b).

Figure S9. Rietveld refinement plots for $Fe_2P_2O_7$ obtained by calcination under N_2 at 700 °C of **Fe-HPAA** (a) and **Fe-NH_3-72h** (b).

Figure S10. Plots of the complex impedance plane for **Fe-NH_3-xh** derivatives at 95% RH and various temperatures: 80 (black), 70 (red), 60 (green), 50 (blue), 40 (cyan), 30 (magenta) and 25 °C (yellow).

Figure S11. Plots of the complex impedance plane for **$Fe_{0.41}Zn_{0.59}$-NH_3-xh** and **$Fe_{0.71}Zn_{0.29}$-NH_3-xh** derivatives at 95% RH and various temperatures: 80 (black), 70 (red), 60 (green), 50 (blue), 40 (cyan), 30 (magenta) and 25 °C (yellow).

Figure S12. FTIR spectra for compounds **Fe-HPAA** (a) and **Fe-NH_3-72h** (b).

Figure S13. Size distribution by intensity for compounds **Fe-HPAA** (a) and **Fe-NH_3-72h** (b).

Figure S14. Size distribution by intensity before (a, c) and post impedance (b, d) measurements for **$Fe_{0.41}Zn_{0.59}$-HPAA** (a, b) and **$Fe_{0.41}Zn_{0.59}$-NH_3-1h** (c, d).

Figure S15. Size distribution by intensity for **$Fe_{0.71}Zn_{0.29}$-HPAA** (a) and **$Fe_{0.71}Zn_{0.29}$-NH_3-5h** (b) before and post impedance measurements.

Figure S16. Time evolution of total iron, phosphorus and zinc leached for the photocatalytic reactions of (a) **phenol** and **$Fe_{0.71}Zn_{0.29}$-HPAA** under visible irradiation, **4-chlorophenol** and **Fe-HPAA** (b) under visible and (c) UVA irradiation, (d) **methylene blue** and **Fe-HPAA** under UVA irradiation.

Figure S17. Mössbauer absorption spectra for **Fe-HPAA** solids: (green) as-synthesized; (red) spent photocatalyst after phenol photodegradation in the presence of UVA light; (blue) **Fe-HPAA** as-synthesized (from an acetate-buffered $FeSO_4\cdot 7H_2O$ + HPAA solution) at 100 °C; (black) as-synthesized at 140 °C.

Figure S18. Time evolution of TOC removal for phenol degradation with **Fe-HPAA** under visible light for different cycles: first (orange) and second (olive).

Figure S19. X-ray powder diffraction patterns for as-synthesized **Fe-HPAA** (red) and after photocatalytic test under visible irradiation (black).

Tables:

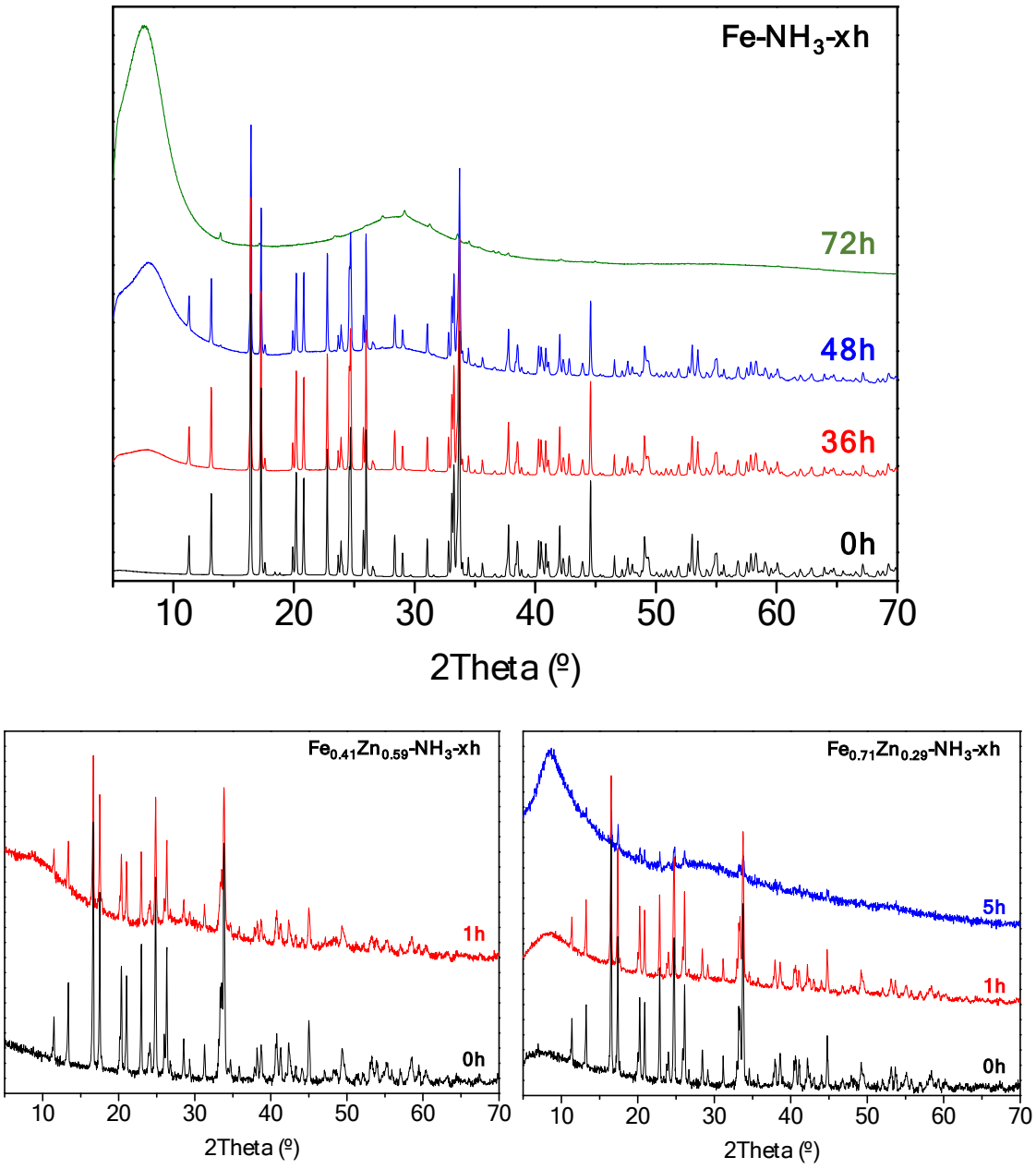

Figure S1. X-ray powder diffraction patterns for **Fe-NH_3-xh**, **$Fe_{0.41}Zn_{0.59}$-NH_3-xh** and **$Fe_{0.71}Zn_{0.29}$-NH_3-xh** derivatives.

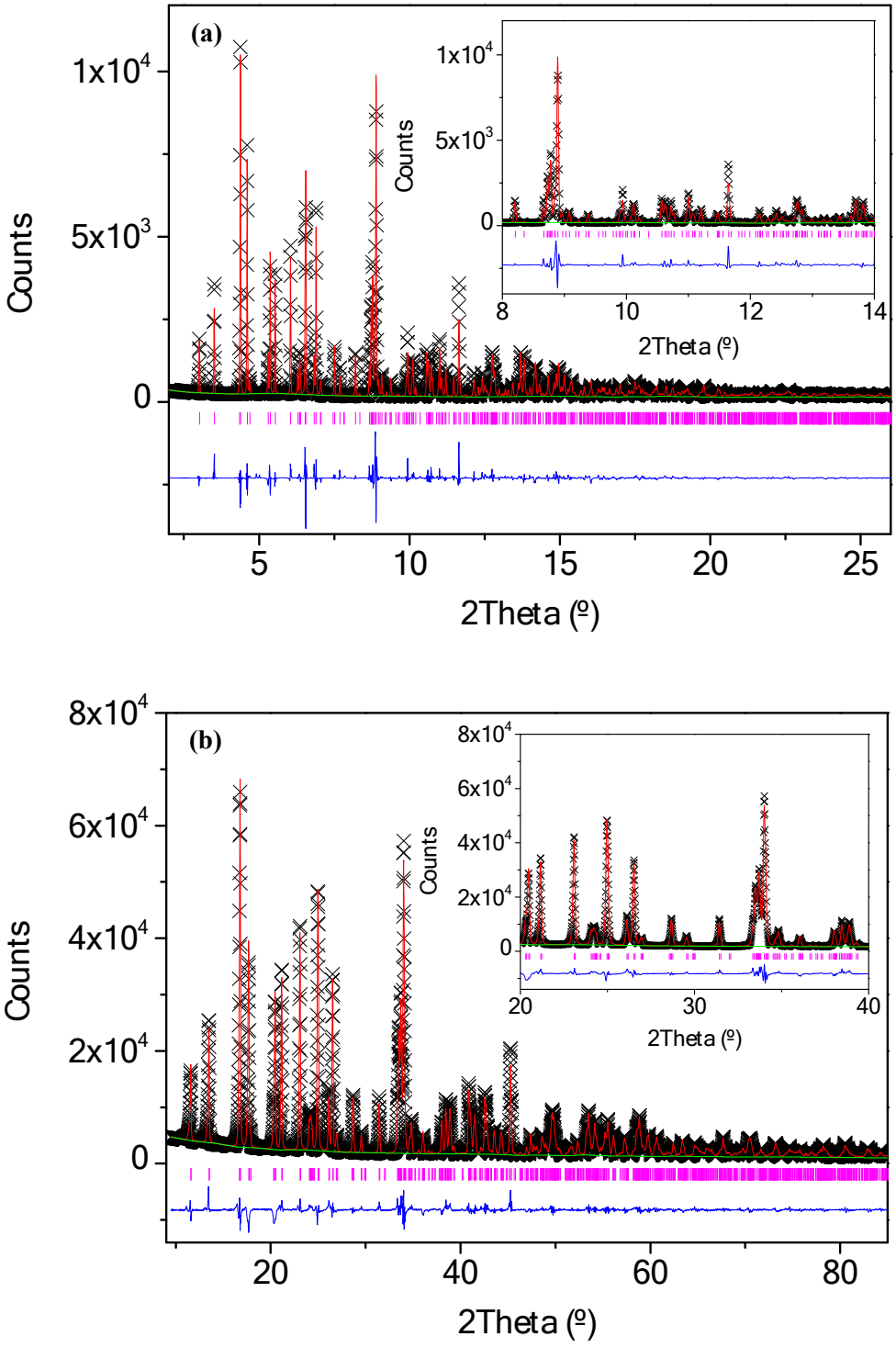

Figure S2. XRPD Rietveld plots for **Fe-HPAA** (a) and **Zn-HPAA** (b).

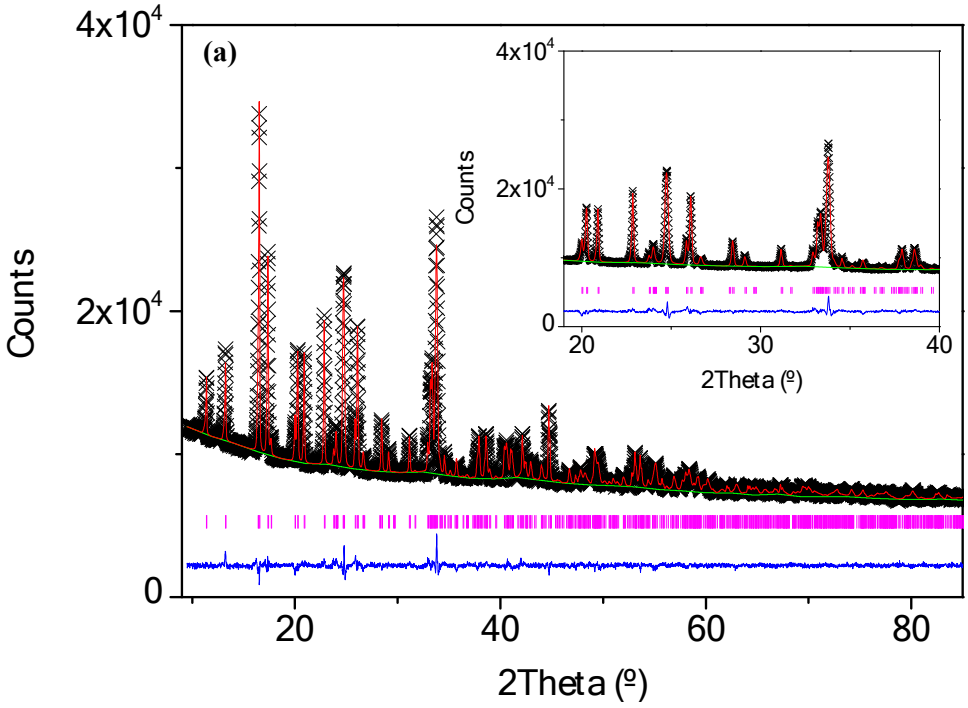
(a)
4x10^4
2x10^4
0
Counts
20
40
60
80
2Theta (º)
4x10^4
2x10^4
0
Counts
20
30
40
2Theta (º)

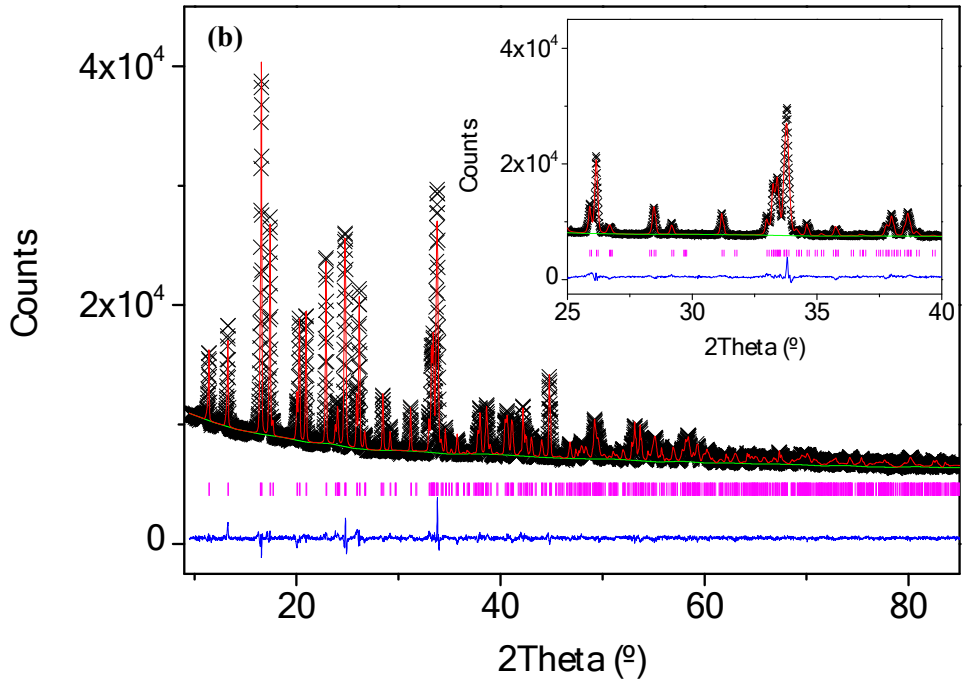
(b)
4x10^4
2x10^4
0
Counts
20
40
60
80
2Theta (º)
4x10^4
2x10^4
0
Counts
25
30
35
40
2Theta (º)

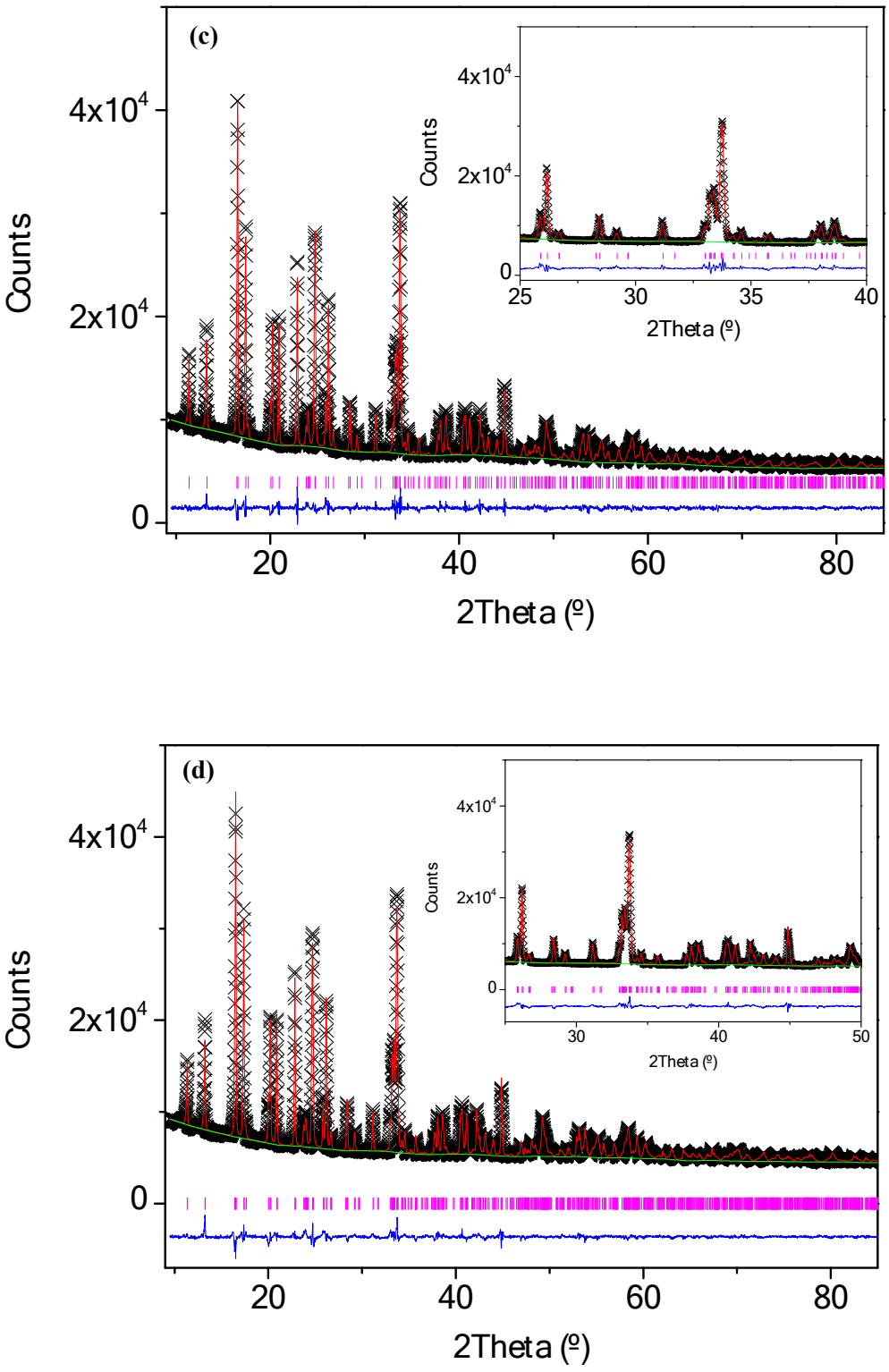

Figure S3. Final Rietveld plots for **$Fe_{0.89}Zn_{0.11}$-HPAA** (a), **$Fe_{0.71}Zn_{0.29}$-HPAA** (b), **$Fe_{0.54}Zn_{0.46}$-HPAA** (c) and **$Fe_{0.41}Zn_{0.59}$-HPAA** (d).

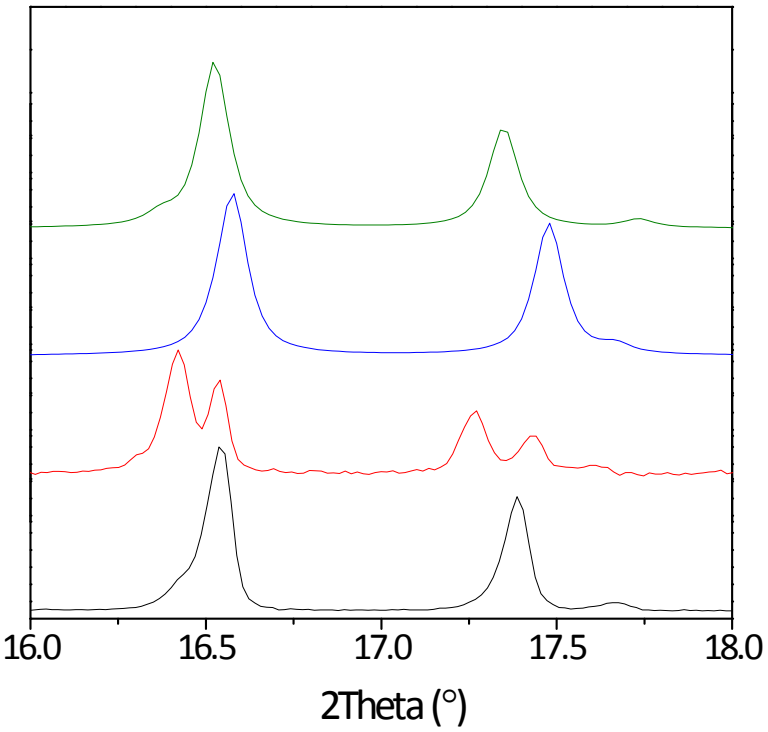

Figure S4. XRD pattern comparison of physical mixture of **Fe-HPAA/Zn-HPAA** (70/30 % w/w) and bimetallic systems in the 16-18° angular region (**Fe-HPAA**, green line; **Zn-HPAA**, blue line, mixture **Fe-HPAA/Zn-HPAA**, red line and **$Fe_{0.71}Zn_{0.29}$-HPAA**, black line).

(a)

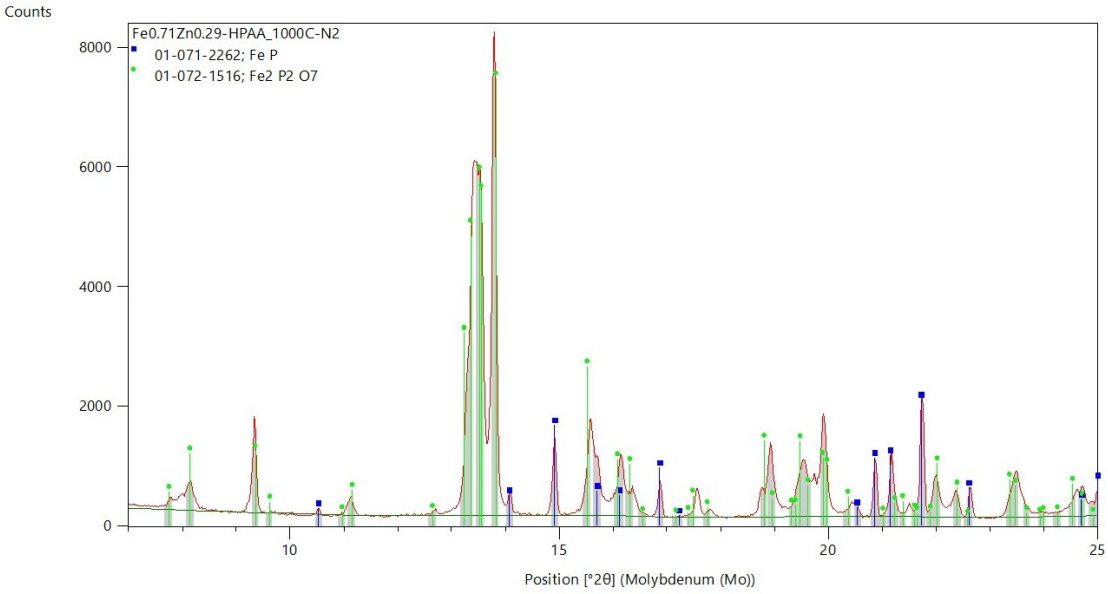

(b)

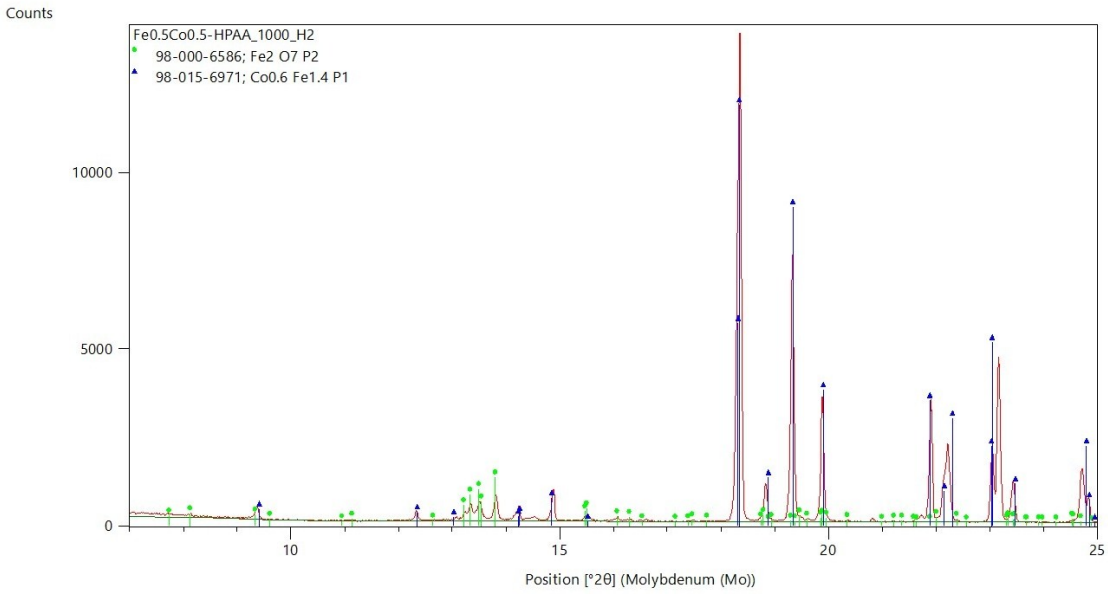

Figure S5. Phase identification for compounds **Fe_xM_{1-x}-HPAA** (M^{2+}=Co, Zn) calcined at 1000 °C under (a) N_2 or (b) H_2 atmospheres.

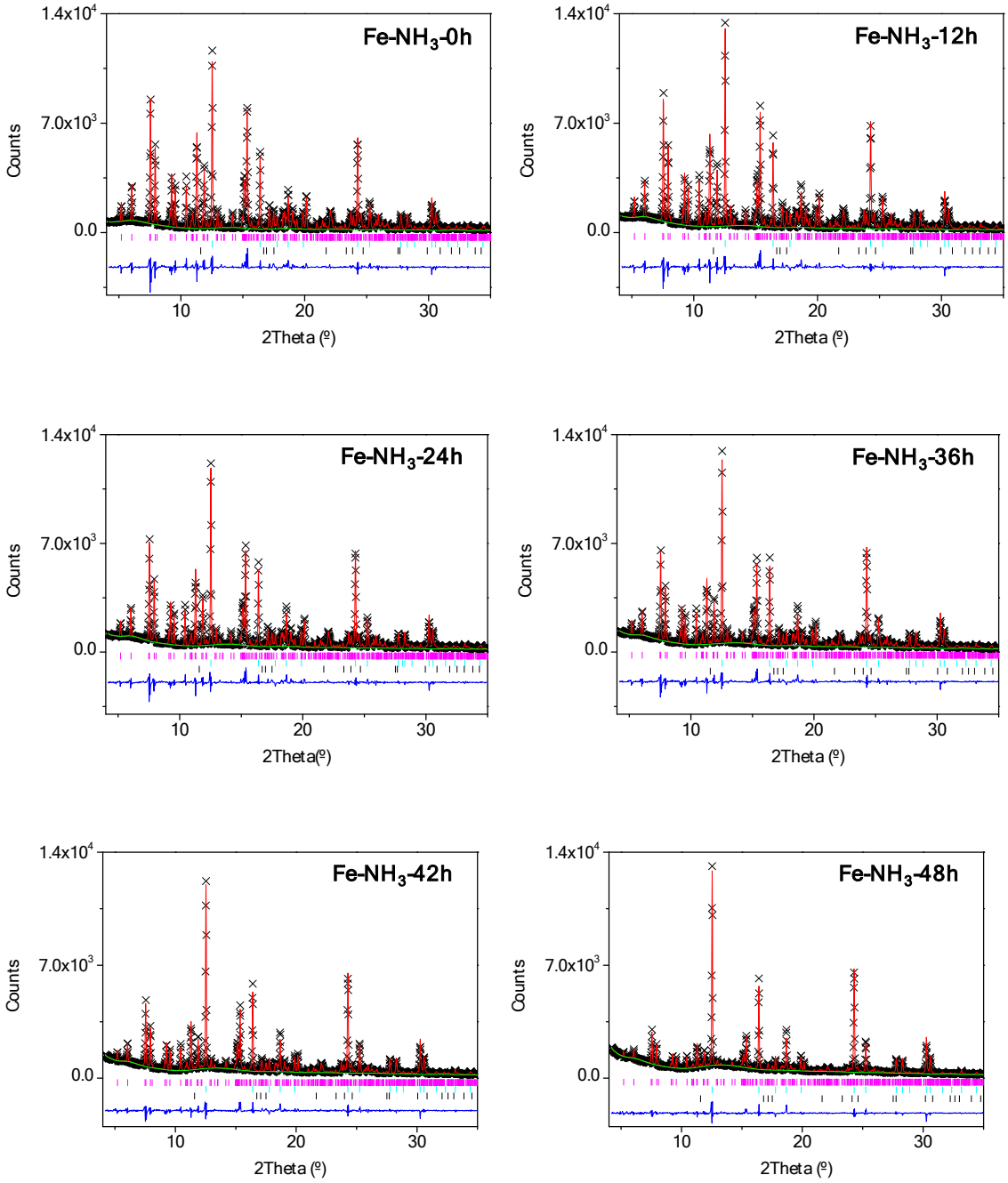

Figure S6. Rietveld plots for **$Fe[HO_3PCH(OH)CO_2]\cdot(NH_3)_x\cdot(H_2O)_y$ (Fe-NH_3-xh).**

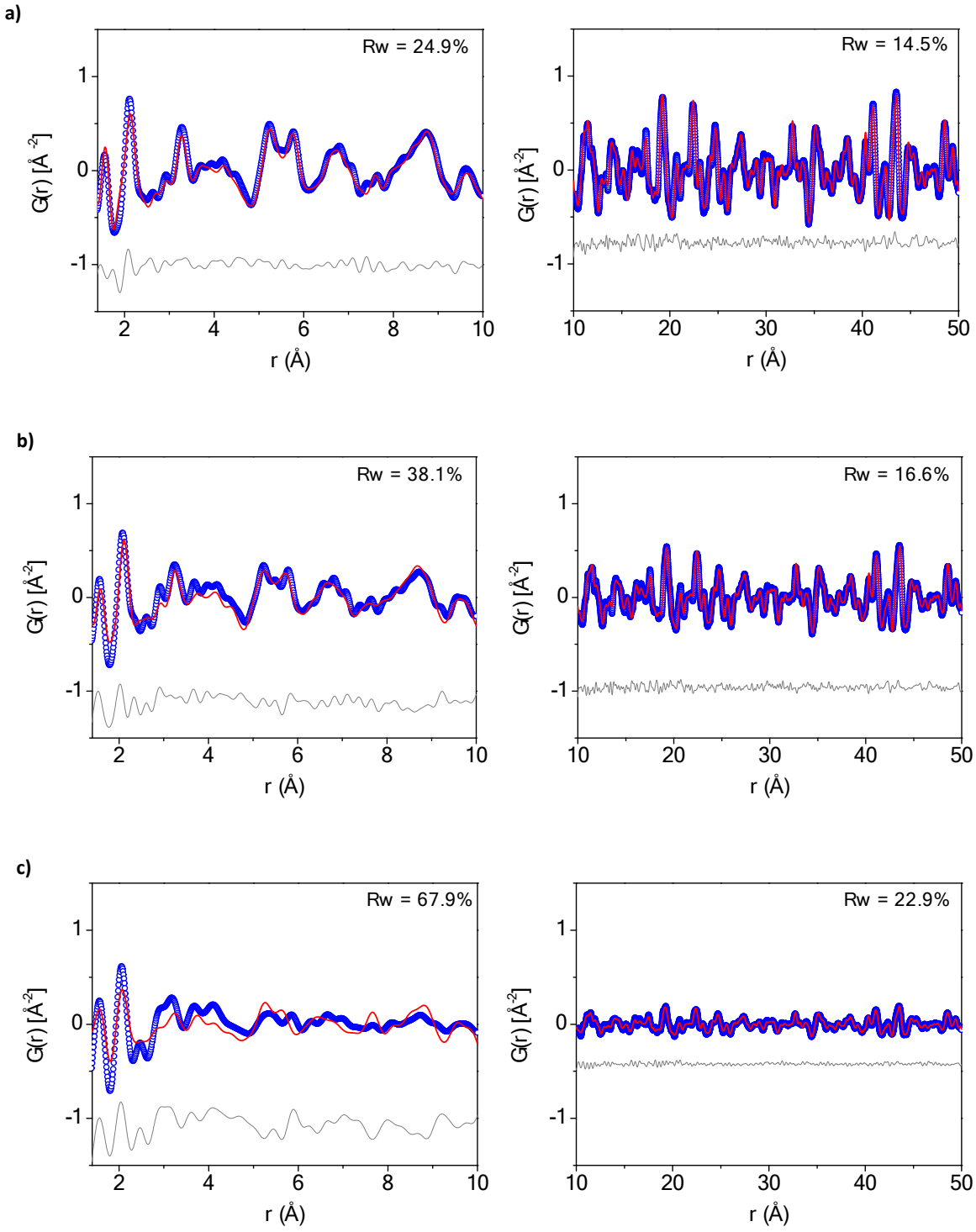

Figure S7. X-ray Pair Distribution Function (PDF) analysis. Observed (blue symbol) and calculated (red line) PDF patterns of **Fe-HPAA** (a), **Fe-NH$_3$-36h** (b), **Fe-NH$_3$-48h** (c) in the range 1.4-10 Å (left) and 10-50 Å (right).

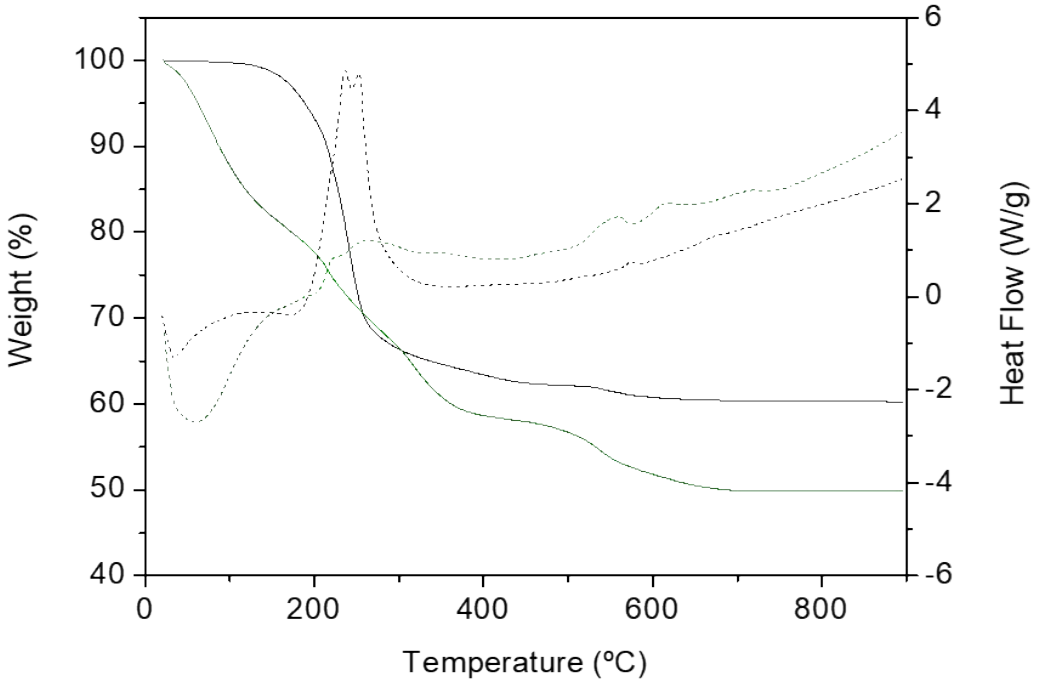

Figure S8. TG and DTA curves for compounds **Fe-HPAA** (a) and **Fe-NH$_3$-72h** (b).

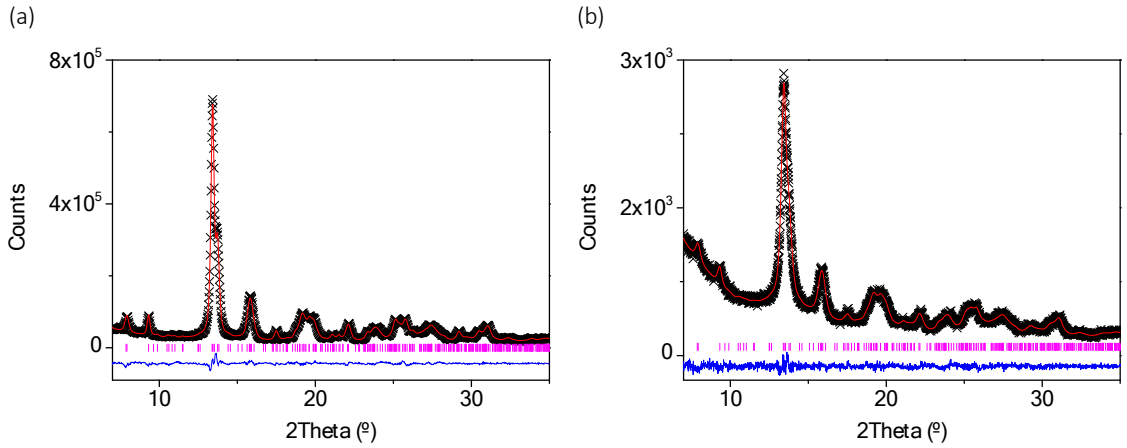

Figure S9. Rietveld refinement plots for $Fe_2P_2O_7$ obtained by calcination under N_2 at 700 °C of **Fe-HPAA** (a) and **Fe-NH$_3$-72h** (b).

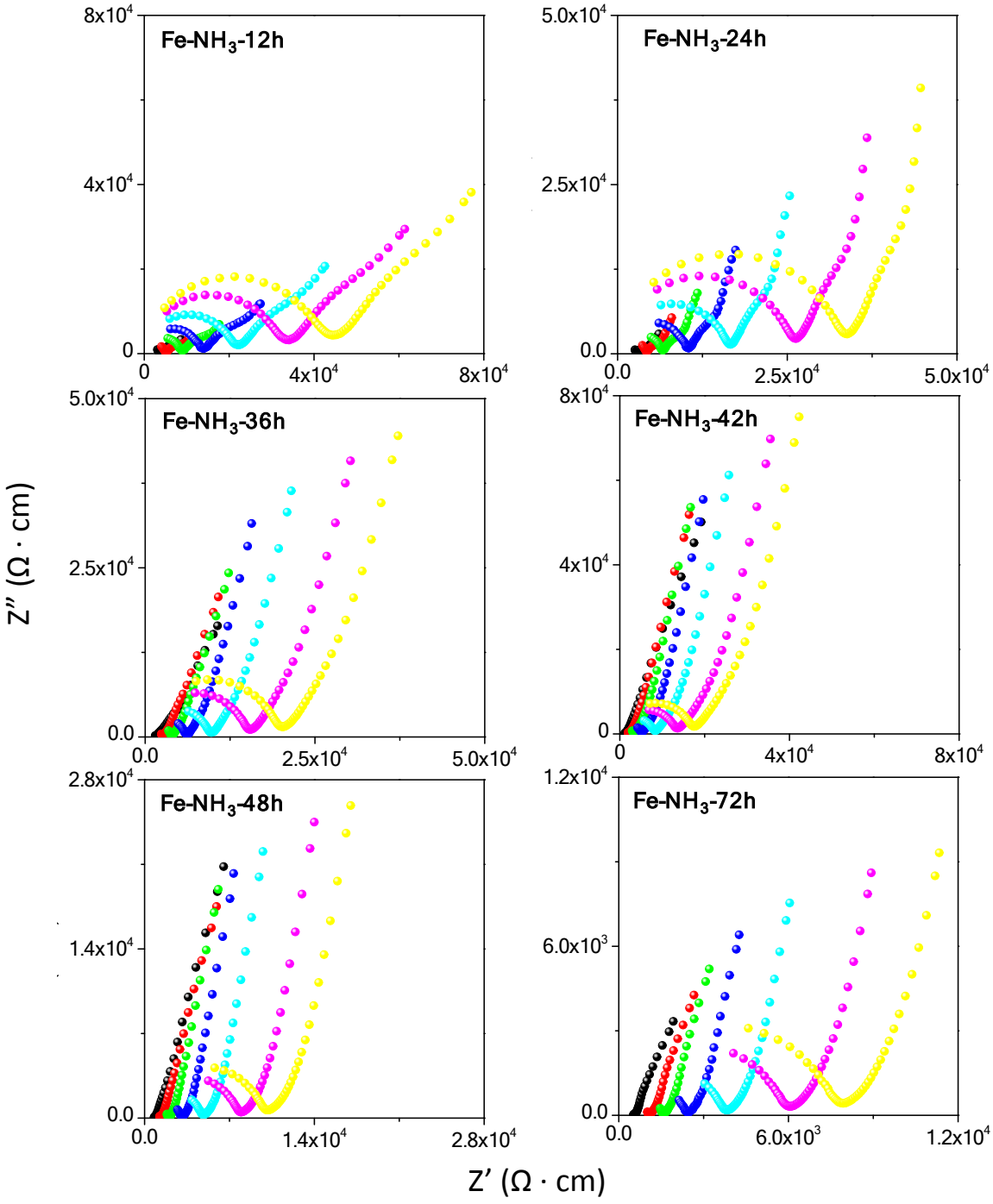

Figure S10. Plots of the complex impedance plane for **Fe-NH$_3$-xh** derivatives at 95% RH and various temperatures: 80 (black), 70 (red), 60 (green), 50 (blue), 40 (cyan), 30 (magenta) and 25 °C (yellow).

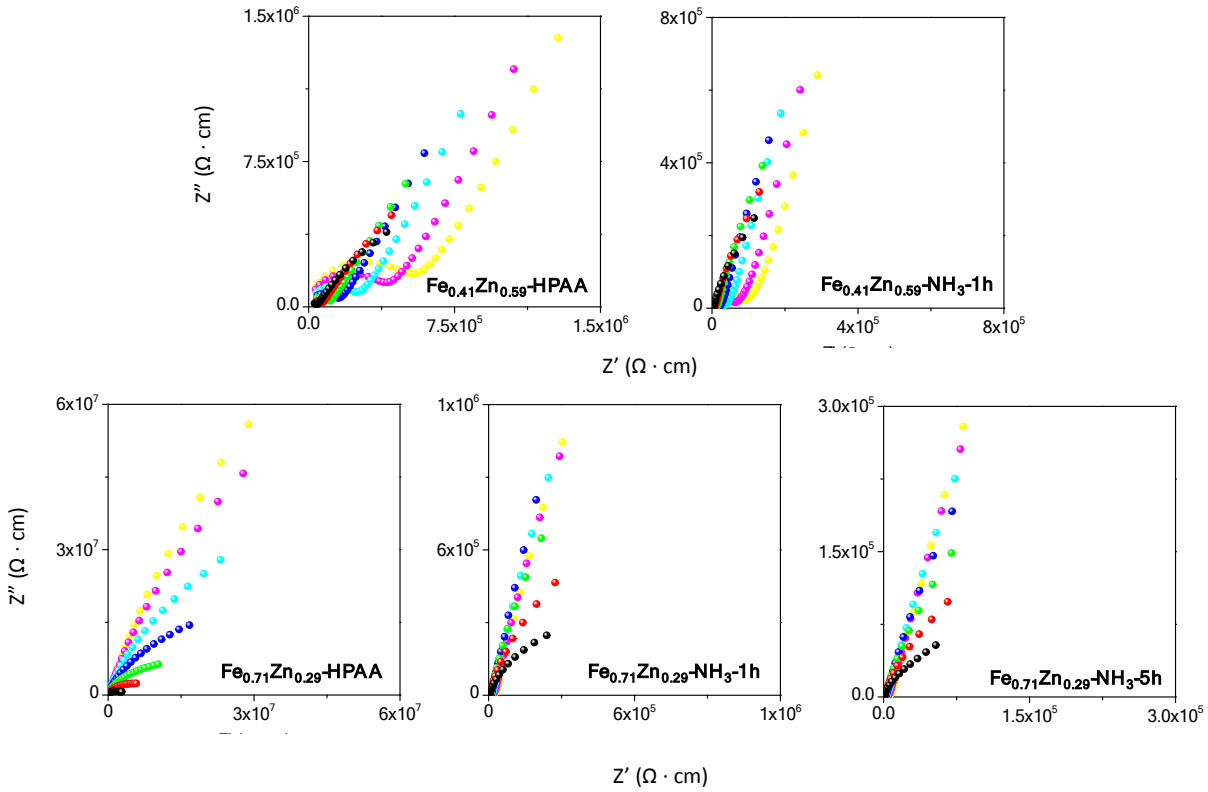

Figure S11. Plots of the complex impedance plane for **$Fe_{0.41}Zn_{0.59}$-NH_3-xh** and **$Fe_{0.71}Zn_{0.29}$-NH_3-xh** derivatives at 95% RH and various temperatures: 80 (black), 70 (red), 60 (green), 50 (blue), 40 (cyan), 30 (magenta) and 25 °C (yellow).

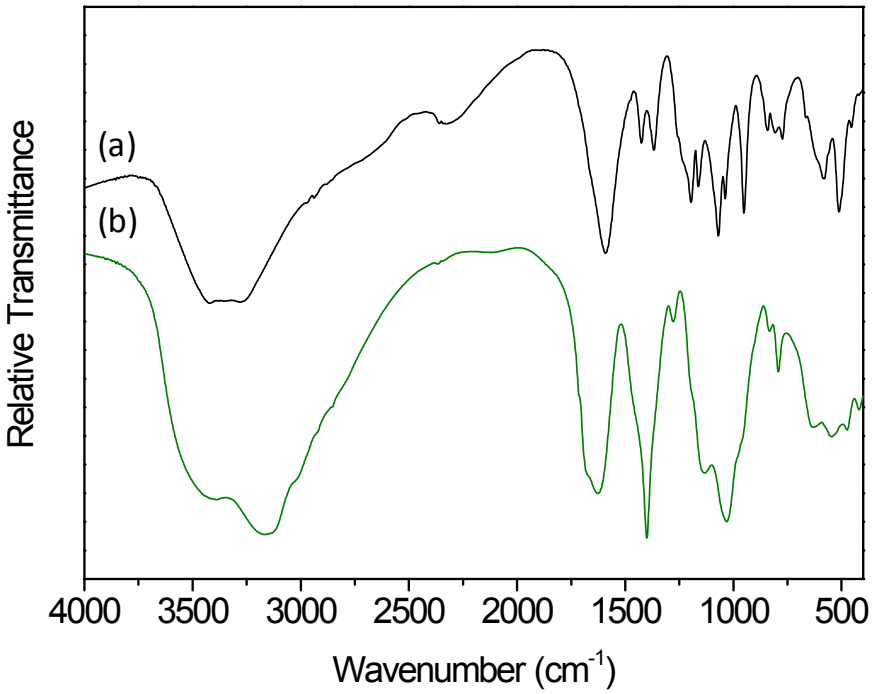

Figure S12. FTIR spectra for compounds **Fe-HPAA** (a) and **Fe-NH_3-72h** (b).

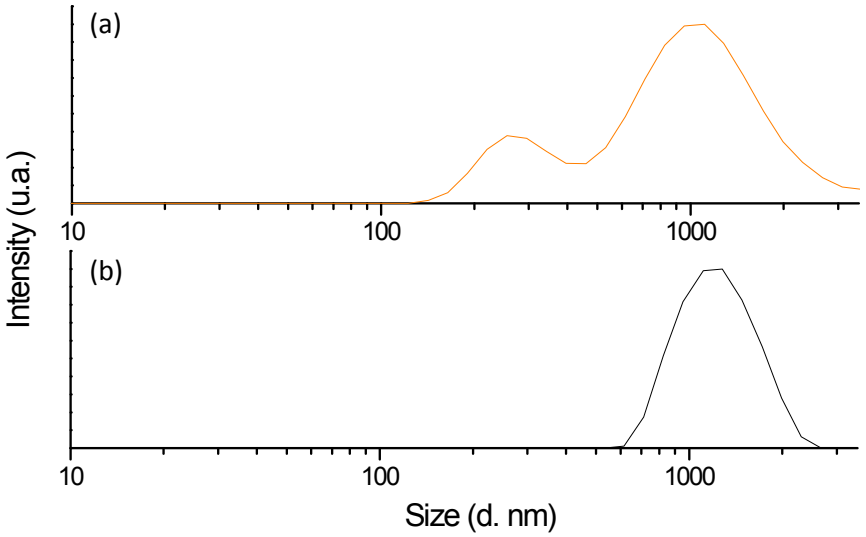

Figure S13. Size distribution by intensity for compounds **Fe-HPAA** (a) and **Fe-NH$_3$-72h** (b).

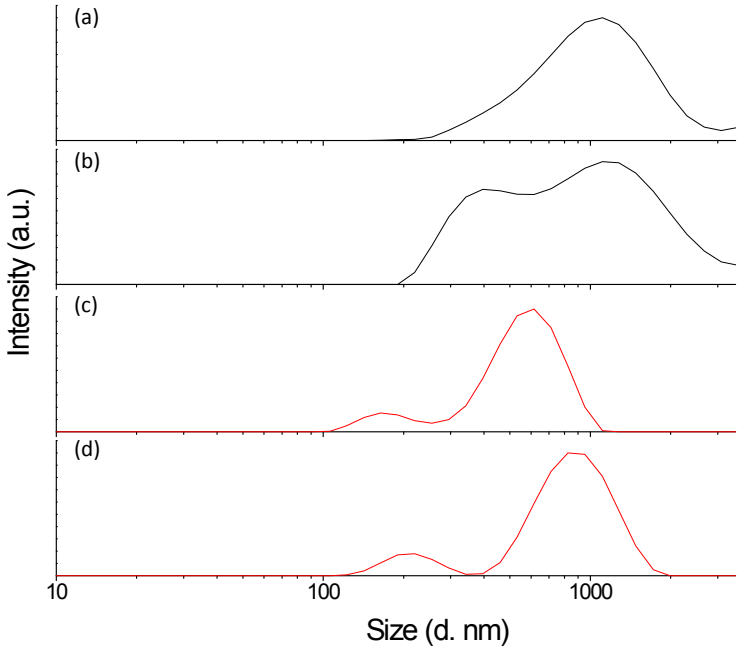

Figure S14. Size distribution by intensity before (a, c) and post impedance (b, d) measurements for **Fe$_{0.41}$Zn$_{0.59}$-HPAA** (a, b) and **Fe$_{0.41}$Zn$_{0.59}$-NH$_3$-1h** (c, d).

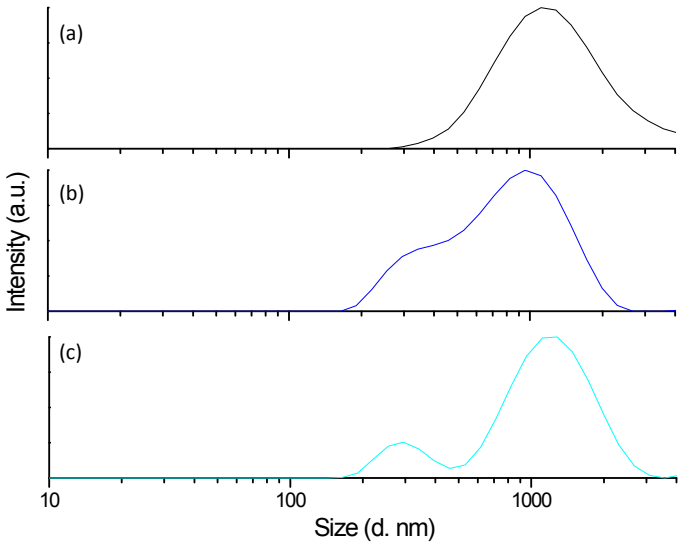

Figure S15. Size distribution by intensity for **$Fe_{0.71}Zn_{0.29}$-HPAA** (a) and **$Fe_{0.71}Zn_{0.29}$-NH_3-5h** (b) before and post impedance measurements.

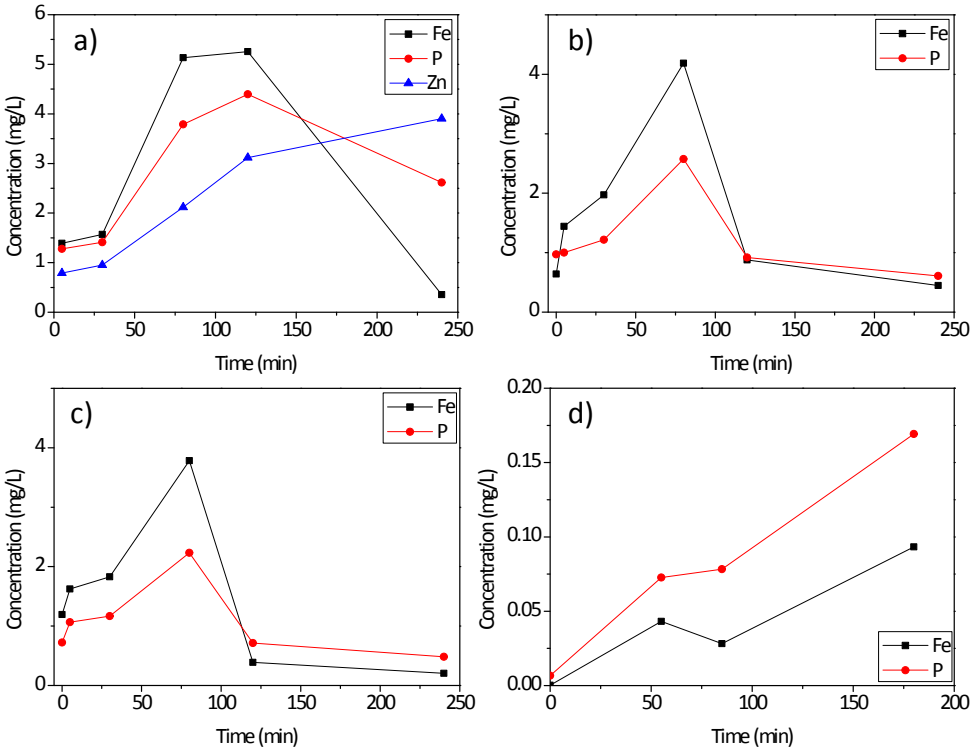

Figure S16. Time evolution of total iron, phosphorus and zinc leached for the photocatalytic reactions of (a) **phenol** and **$Fe_{0.71}Zn_{0.29}$-HPAA** under visible irradiation, **4-chlorophenol** and **Fe-HPAA** (b) under visible and (c) UVA irradiation, (d) **methylene blue** and **Fe-HPAA** under UVA irradiation.

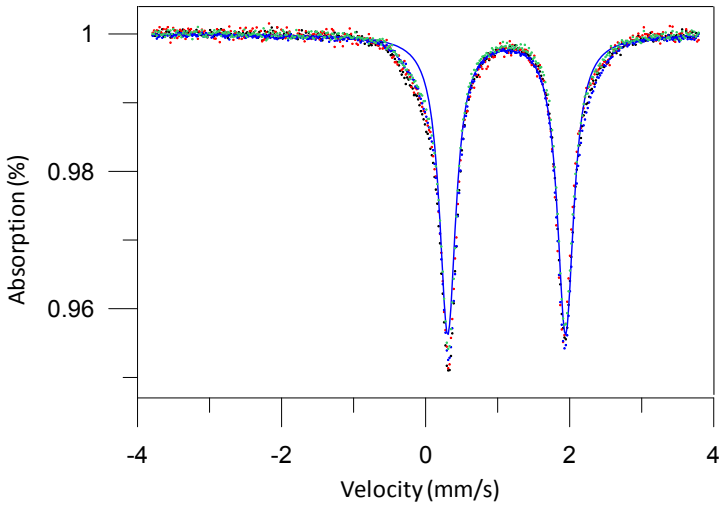

Figure S17. Mössbauer absorption spectra for **Fe-HPAA** solids: (green) as-synthesized; (red) spent photocatalyst after phenol photodegradation in the presence of UVA light; (blue) **Fe-HPAA** as-synthesized (from an acetate-buffered $FeSO_4 \cdot 7H_2O$ + HPAA solution) at 100 °C; (black) as-synthesized at 140 °C.

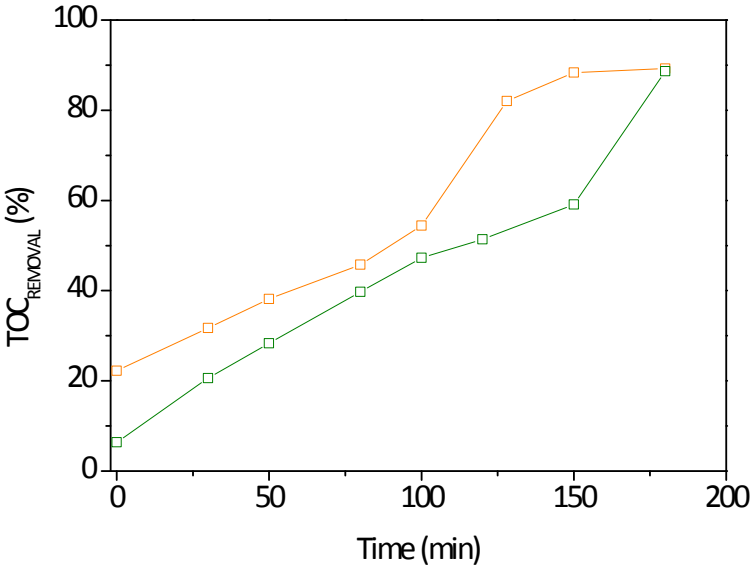

Figure S18. Time evolution of TOC removal for phenol degradation with **Fe-HPAA** under visible light for different cycles: first (orange) and second (olive).

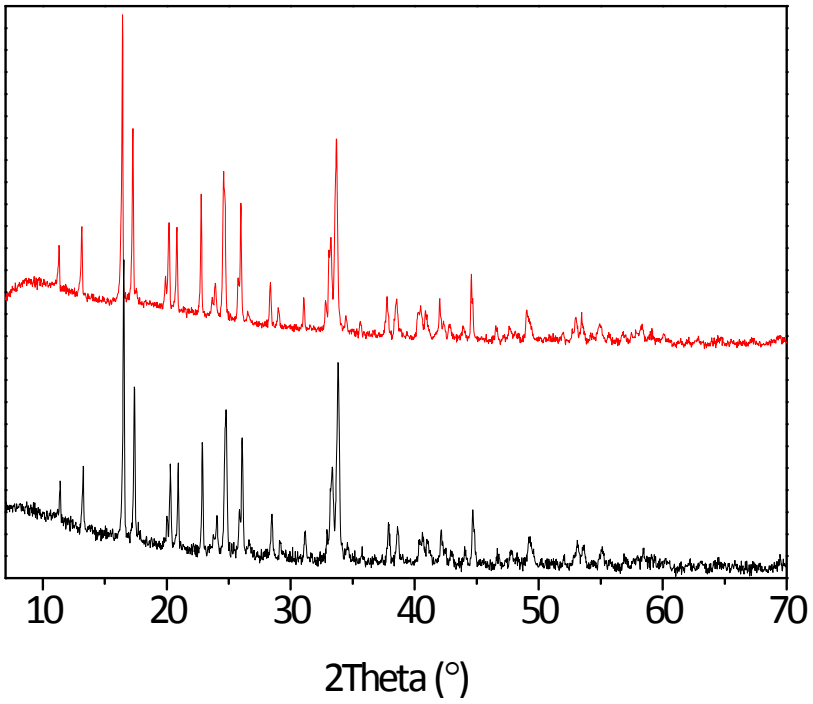

Figure S19. X-ray powder diffraction patterns for as-synthesized **Fe-HPAA** (red) and after photocatalytic test under visible irradiation (black).

Table S1. Elemental analysis and stoichiometries for compounds **Fe-NH_3-xh** and **Fe_xZn_{1-x}-NH_3-xh.**

Sample	Exposure time (xh)	%C		%H		%N		Stoichiometry
		Found	Calc.	Found	Calc.	Found	Calc.	
Fe-NH_3-xh	12	9.046	9.300	3.147	3.356	1.071	1.085	$Fe(HO_3PCHOHCOO)(H_2O)_{2.5}(NH_3)_{0.2}$
	24	8.967	9.179	3.285	3.543	1.953	2.141	$Fe(HO_3PCHOHCOO)(H_2O)_{2.5}(NH_3)_{0.4}$
	36	8.638	8.974	3.587	3.860	3.777	3.925	$Fe(HO_3PCHOHCOO)(H_2O)_3(NH_3)_{0.75}$
	42	8.669	8.946	3.595	3.904	4.257	4.173	$Fe(HO_3PCHOHCOO)(H_2O)_3(NH_3)_{0.8}$
	48	8.340	8.423	3.838	4.506	5.998	6.139	$Fe(HO_3PCHOHCOO)(H_2O)_3(NH_3)_{1.25}$
	72	7.615	8.179	4.629	4.890	8.796	8.346	$Fe(HO_3PCHOHCOO)(H_2O)_3(NH_3)_{1.75}$
$Fe_{0.71}Zn_{0.29}$-NH_3-xh	1	8.634	8.699	3.520	3.942	3.007	3.044	$Fe_{0.71}Zn_{0.29}(HO_3PCHOHCOO)(H_2O)_3(NH_3)_{0.6}$
	5	7.912	8.242	4.435	4.669	7.227	7.209	$Fe_{0.71}Zn_{0.29}(HO_3PCHOHCOO)(H_2O)_3(NH_3)_{1.5}$
$Fe_{0.41}Zn_{0.59}$-NH_3-xh	1	8.164	8.236	4.083	4.458	6.264	6.243	$Fe_{0.41}Zn_{0.59}(HO_3PCHOHCOO)(H_2O)_3(NH_3)_{1.3}$

Table S2. Selected crystallographic data for compounds **Fe-HPAA**, **Zn-HPAA** and **Fe_xZn_{1-x}-HPAA**.

Phase	**Fe-HPAA**	**$Fe_{0.89}Zn_{0.11}$-HPAA**	**$Fe_{0.71}Zn_{0.29}$-HPAA**	**$Fe_{0.54}Zn_{0.46}$-HPAA**	**$Fe_{0.41}Zn_{0.59}$-HPAA**	**Zn-HPAA**	**$Fe_2P_2O_7$**
Space group	P 2_1/c	P 2_1/c	P 2_1/c	P 2_1/c	P 2_1/c	P 2_1/c	B 2_1/c
Chemical formula	C_2FeO_8P	$C_2Fe_{0.89}Zn_{0.11}O_8P$	$C_2Fe_{0.71}Zn_{0.29}O_8P$	$C_2Fe_{0.54}Zn_{0.46}O_8P$	$C_2Fe_{0.41}Zn_{0.59}O_8P$	C_2ZnO_8P	$Fe_2P_2O_7$
Formula mass ($g \cdot mol^{-1}$)	238.83	239.88	241.60	243.22	244.46	248.37	285.64
λ (Å)	0.4124	1.5418	1.5418	1.5418	1.5418	1.5418	0.7093
a (Å)	5.7580(1)	5.7508(1)	5.75004(9)	5.74238(9)	5.74322(8)	5.72097(9)	13.298(5)
b (Å)	15.6192(3)	15.5825(3)	15.5733(2)	15.5573(3)	15.5598(2)	15.5342(2)	8.437(3)
c (Å)	7.8938(1)	7.8847(2)	7.8849(2)	7.8745(2)	7.8722(1)	7.8516(1)	8.993(3)
β (º)	109.707(1)	109.745(1)	109.869(1)	109.985(1)	110.1420(9)	110.3112(9)	104.24(1)
Unit cell volume ($Å^3$)	668.35(3)	665.02(3)	664.04(2)	661.12(3)	660.47(2)	654.3(2)	978.0(10)
Z	4	4	4	4	4	4	8
No. of independent reflections	1148	707	706	703	703	697	312
Data/Restrains/ Parameters	954/19/75	6191/19/82	1106/19/82	573/19/89	1118/19/46	1102/19/95	433/31/77
R_{WP}	0.0996	0.0139	0.0165	0.0194	0.0230	0.0650	0.0486
R_P	0.0714	0.0102	0.0117	0.0140	0.0162	0.0493	0.0378
R_F	0.0722	0.0644	0.0614	0.0470	0.0491	0.0495	0.0130

Table S3. Chemical composition for compounds **Fe_xM_{1-x}-HPAA** (M = Mn^{2+}, Co^{2+} and Zn^{2+}).

Nominal $[Fe^0+Fe^{2+}]/Zn^{2+}$	**Chemical composition**
0.92 : 0.08	$Fe_{0.89}Zn_{0.11}(HO_3PCHOHCOO)(H_2O)_{2.5}$
0.79 : 0.21	$Fe_{0.71}Zn_{0.29}(HO_3PCHOHCOO)(H_2O)_{2.5}$
0.68 : 0.32	$Fe_{0.54}Zn_{0.46}(HO_3PCHOHCOO)(H_2O)_{2.5}$
0.55 : 0.45	$Fe_{0.41}Zn_{0.59}(HO_3PCHOHCOO)(H_2O)_{2.5}$
Nominal $[Fe^0+Fe^{2+}]/Co^{2+}$	**Chemical composition**
0.79 : 0.21	$Fe_{0.78}Co_{0.22}(HO_3PCHOHCOO)(H_2O)_{2.5}$
0.68 : 0.32	$Fe_{0.66}Co_{0.34}(HO_3PCHOHCOO)(H_2O)_{2.5}$
0.55 : 0.45	$Fe_{0.59}Co_{0.41}(HO_3PCHOHCOO)(H_2O)_{2.5}$
Nominal $[Fe^0+Fe^{2+}]/Mn^{2+}$	**Chemical composition**
0.92 : 0.08	$Fe_{0.85}Mn_{0.15}(HO_3PCHOHCOO)(H_2O)_{2.5}$
0.79 : 0.21	$Fe_{0.8}Mn_{0.2}(HO_3PCHOHCOO)(H_2O)_{2.5}$

Table S4. XPS Fe(II)/Fe(III) atomic ratio.

Catalyst		**Pollutant**	**Radiation**	**Fe(II)**	**Fe(III)**	**Fe(II)/Fe(III)**
Fe-HPAA	As synthesized	Phenol	Visible	61.9%	38.1%	1.62
	After a photocatalytic test			49.0%	51.0%	0.96
	As synthesized	Methylene blue	UVA	56.8%	43.2%	1.32
	After a photocatalytic test			50.3%	49.7%	1.01
$Fe_{0.71}Zn_{0.29}$-HPAA	As synthesized	Phenol	Visible	66.1%	33.9%	1.95
	After a photocatalytic test			51.8%	48.2%	1.07
	As synthesized	Methylene blue	UVA	72.9%	27.1%	2.69
	After a photocatalytic test			69.2%	30.8%	2.24